

# DELIVERABLE 4.6

## THE AZORES CASE STUDY: COMPARING RISK ANALYSES BASED ON SHIPPING DENSITY AND ACOUSTIC MODELLING



<b>Work Package</b>	RAGES Work Package 4 Deliverable 4.6 (Additional Deliverable).
<b>Authors</b>	Okeanos R&D Centre, University of the Azores & IMAR – Institute of Marine Research: Mónica A. Silva, Irma Cascão MarSensing Lda; Sérgio M. Jesus LARSyS, University of Algarve: Cristiano Soares
<b>Version</b>	FINAL
<b>Date</b>	June 2021
<b>Citation</b>	Silva, M.A., Cascão, I., Romagosa, M., Soares C., Jesus, S.M. (2021). The Azores case study: comparing risk analyses based on shipping density and acoustic modelling. Report to RAGES Project – WP4: Applying the RAGES Risk-Based Approach to MSFD Descriptor 11, Underwater Noise, 15 pp + 1 annex.

## Preface

The main goal of the Azores case study was to compare the results of a spatially explicit risk analysis of continuous anthropogenic noise on cetaceans based on shipping density data (*proxy* of noise in the subregional approach) to those based on acoustic modelling. The development of a shipping noise model for part of the archipelago enabled assessing the agreement between: i) the spatial distribution of noise predictions and shipping traffic, and ii) risk maps for cetaceans computed from noise predictions with those derived from shipping density data alone. This work does not follow the RAGES risk approach, however the results of the study add to the knowledge base and increase our knowledge as to the interpretation of shipping data.

# Table of Contents

Preface .....	2
1. The Azores shipping noise model .....	4
2.1 Shipping noise modelling .....	4
2.2 Wind noise modelling .....	4
2. Ship Noise Excess .....	4
3. Risk Index .....	4
4. Comparing pressure and risk indicators based on shipping density and on acoustic modelling .....	5
5. Comparison of pressure indicators .....	5
6. Comparison of risk indicators .....	9
7. Lessons learned and Recommendations .....	13
8. References .....	14

## 1. The Azores shipping noise model

### 2.1 Shipping noise modelling

Shipping noise modelling was performed by Marsensing within project JONAS and details are provided in Soares et al. (2020a, b) and Jesus et al. (in prep).

In brief, vessel positions were derived from satellite AIS (sAIS) data sourced by AIShub (<https://www.aishub.net/>) for the area around the central islands of the Azores for June 2018. Data were sourced with a spatial resolution of 500×500 m and a temporal resolution of 10 min. Stationary vessels were removed from the dataset. From this, shipping density was calculated as the  $\log_{10}$  of the number of ship hours per square arc minute (arc min). Bathymetric data were extracted from the General Bathymetric Chart of Oceans database ([www.gebco.net](http://www.gebco.net)) (GEBCO 2020). Temperature and salinity data were taken from models provided by CMEMS (<https://marine.copernicus.eu/>). Sound speed profile was calculated from the salinity, temperature and depth data using Mackenzie (1981) nine-term equation. Seabed acoustic parameters were those of Soares et al. (2015) and Maglio et al. (2015) assuming a two layer bottom model composed of a fluid sandy sediment layer over a rocky semi-infinite sub-bottom. Source levels of different ships were obtained by McKenna et al. (2012). In the case of sailing vessels, for which there are no source levels available in the literature, a source level of 1% of the cargo source level (~20 dB) was used. Computation of the sound field for each position of each vessel was done using the Kraken propagation model (Porter & Reiss 1984, Kuperman et al. 1991), set up with the bathymetry, water column and seabed parameters. Shipping noise (SPL, in dB re 1  $\mu$ Pa) was calculated for the 40-1000 Hz frequency band at 10, 200 and 484m depth. The power average of shipping noise at these three depths was also calculated.

### 2.2 Wind noise modelling

Wind speed data were retrieved from the European Centre for Medium-Range Weather Forecast (ECMWF) for the whole month of June 2018 with a spatial resolution of 45x45 arc min and a temporal resolution of 3h. Wind speed was input into the Kewley and Carey (KC) model to estimate wind driven ocean surface generated ambient sound using 1/3 octave centre frequencies throughout the 20-1000 Hz band for the whole area of interest.

Predictions from the shipping noise model were compared and found to agree reasonably well with concurrent field measurements at different locations within the study area (not shown here). Therefore, the noise model provides satisfactory predictions of underwater noise in the area and may be used as a risk assessment tool (Soares et al. 2020a).

## 2. Ship Noise Excess

Ship noise excess (ENL, expressed in dB; Merchant et al. 2018a) provides a quantitative measure of the pressure of continuous anthropogenic sound and currently is an OSPAR candidate indicator of ambient noise (van Oostveen et al. 2020). ENL was calculated by first adding the wind noise layer and the ship noise layer to produce a prediction of the total noise level, and then subtracting the wind noise from the total noise, to obtain an estimate of the excess level of ship noise above wind noise (Farcas et al. 2020). The calculation was performed from the estimated distributions of shipping noise and wind noise at 10-min intervals (yielding 4318 frames for the month) for each one-third octave frequency band centred in the interval 40–1000 Hz (14 centre frequencies) and depth (10, 200, 488 m, average of these depths). The individual time frames were used to calculate the average ENL and the ENL exceeded for 25%, 50% and 75% of the time.

## 3. Risk Index

A risk index (RI) was calculated to determine the distribution and magnitude of coincidence between shipping noise levels and cetacean species (Merchant et al. 2018b). Noise levels were normalized to range from 0 to 1 by dividing the noise value of each cell by the maximum noise level over all cells from the entire map. Cetacean density was normalized in the

same way. RI was then calculated for every cell by multiplying the normalized noise value by the normalized cetacean density. RI was calculated for three cetacean taxa representing different hearing groups (Southall et al. 2019) and depth ranges:

- i) Baleen whales (Balaenopteridae), low-frequency hearing group, shallow divers;
- ii) Atlantic spotted dolphins (*Stenella frontalis*), high-frequency hearing group, shallow divers;
- iii) Sperm whale (*Physeter macrocephalus*), high-frequency hearing group, deep divers.

Density estimates of these taxa were derived from density surface models developed for the central group of islands of the Azores in July-August 2018, based on observations from the MISTIC SEAS II survey (Freitas et al. 2019). RI was computed both for shipping noise level (hereafter RI-SPL) and excess noise level (hereafter RI-ENL) data, calculated as above. SPL and ENL layers were resampled to match the resolution of cetacean density layers (2x2 nm) before calculating the RI. RI values were then mapped to identify areas where higher shipping noise overlaps higher cetacean density.

#### 4. Comparing pressure and risk indicators based on shipping density and on acoustic modelling

sAIS data were mapped to compare the shipping distribution with predictions of SPL and ENL. Shipping density was calculated using the same AIS dataset used to build the noise model as the  $\log_{10}(x+1)$ , where  $x$  is the number of ship hours per 2x2 nm. In addition, to test whether shipping density was a good predictor of shipping noise or excess noise levels, estimates of SPL and ENL for each grid cell 2x2 nm were modelled as a function of the shipping density on that cell.

To compare risk maps calculated from shipping density alone (hereafter RI-shipping) with those based on RI-SPL or RI-ENL, RI was calculated as above, using the normalized value of shipping density multiplied by the normalized density of each cetacean taxa. RI computed from these different approaches were mapped (scaled to 0-100%) to visualize differences in relative risk scores and distribution. Finally, linear and non-linear models were used to investigate the relationship between risk indices computed from shipping density and noise predictions (RI-SPL and RI-ENL).

#### 5. Comparison of pressure indicators

Comparison of predicted ship noise levels and shipping density revealed important differences. It is important to stress that the shipping density layer used in these comparisons is the same layer used in the shipping noise model.

While the maximum shipping density was found east of Terceira island, in the vicinity of the harbours (13 hours of ship time), the highest average SPL was predicted in the channel Faial-Pico (117.3-122.2 dB re 1 $\mu$ Pa), where shipping density was considerably lower (1.2-4.6 hours) but spread over a wider area (Figures 1 & 2a). It is possible that the peak in shipping density in Terceira was associated with slow-moving, therefore less noisy, ship entrances/departures of harbours, or with the traffic of quieter ships. Higher than expected noise levels in the channel might also be due to the influence of shallow bathymetry on acoustic propagation (Figure 2a). The shipping lanes that connect the islands (Figure 1) did not show up as locations of increased SPL; instead, noise was spread out over tens of kms to areas with almost no ship traffic (Figure 2a). Figure 2a also highlights the effect of bathymetry on sound propagation, with bathymetric lines marking locations of sudden changes in SPL. Spatial distribution of average noise was very similar at 10, 200 and 484 m depths, but as expected noise levels decreased with increasing depth (Figures 2a-c). Differences between shipping density and predicted SPL increased as depth increased.

Figure 3 illustrates the relationship between shipping density and predicted average SPL for every grid cell in the study area and at different depths. Average SPL increased non-linearly with shipping density but shipping density explained only a small part (29%) of the variability in SPL data at 10 m depth (Figure 3a), and less than 20% of the variability in SPL data at 200 m and 484 m depth (Figures 3b, c).

The map of median ship noise excess (Figure 4c) at 10 m depth resembled distribution of shipping density more closely than the maps of average ship noise excess (Figures 4a) or average SPL (Figure 2a) at the same depth. This is supported by modelling results (Figure A in Appendix I), which indicate that shipping distribution was a better predictor of median excess noise level than of average ENL or SPL. Conversely, shipping density was a poor proxy for noise levels exceeded for 25% (Figure 4b) and 75% (Figure 4d) of the time.

The maps of average and median ship noise excess were similar (although the latter metric was less influenced by occasional shipping traffic) and comparable to maps of average noise levels (Figures 4a, c & 2a). Average and median ENL surpassed 12 dB in locations with an average SPL >105 dB re 1 $\mu$ Pa. The exception was the area east of Terceira where average and median ship noise excess were 4.2 dB and 0 dB, respectively. The reason for this discrepancy is that wind noise was considerably higher around Terceira than around Faial and Pico and, consequently, level of ship noise above wind noise was lower. Ship noise was likely to exceed the wind noise (by 0-1 dB) 75% of the time. In the channel between Faial and Pico, ship noise excess was 20 dB (reaching 27 dB) for 25% of the month (Figure 4b). For reference, assuming that sound propagates via spherical spreading, a ship noise excess of 20 dB at a particular frequency corresponds to a 10-fold reduction in communication range at that frequency (Hermanssen et al., 2014; Møhl, 1981).

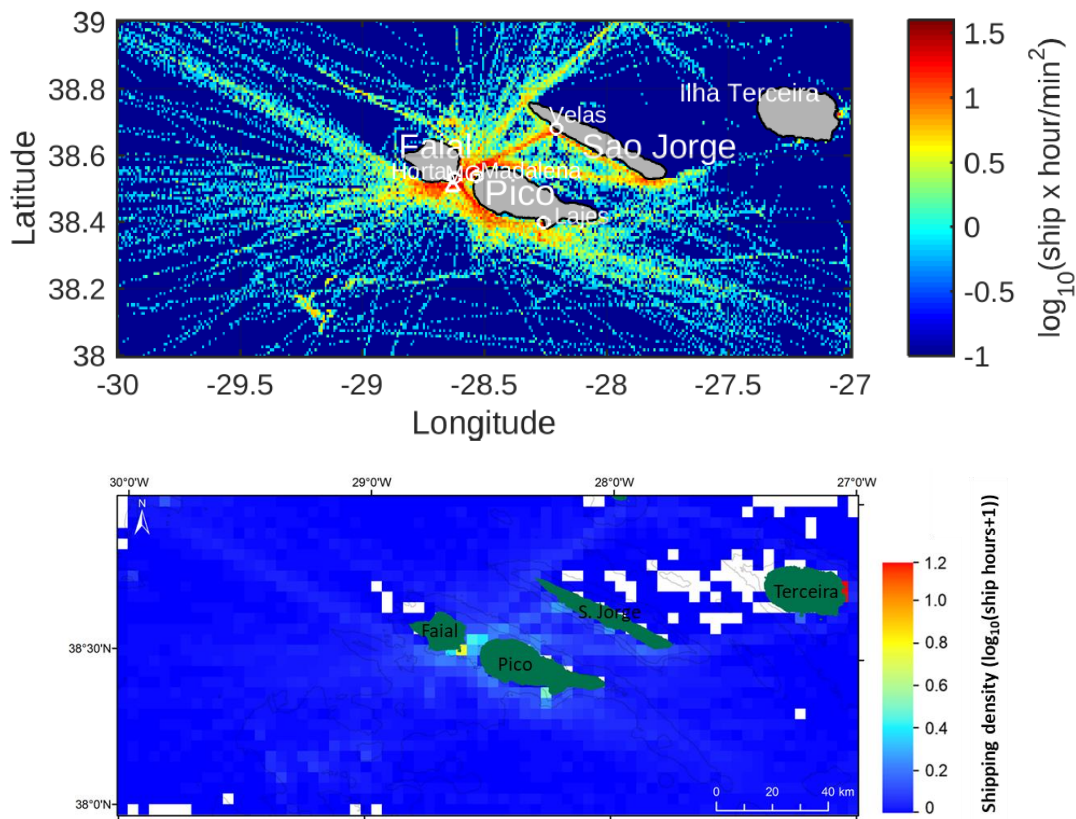


**Figure 1.** Shipping density in  $\log_{10}(\text{ship} \times \text{hour} / \text{arc min}^2)$  based on satellite AIS (sAIS) data for the period 1-30 June 2018 (top). Shipping density transformed [ $\log_{10}(\text{ship} \times \text{hour} + 1)$ ] and rescaled to 2x2nm to match the spatial resolution of cetacean density layer (bottom).

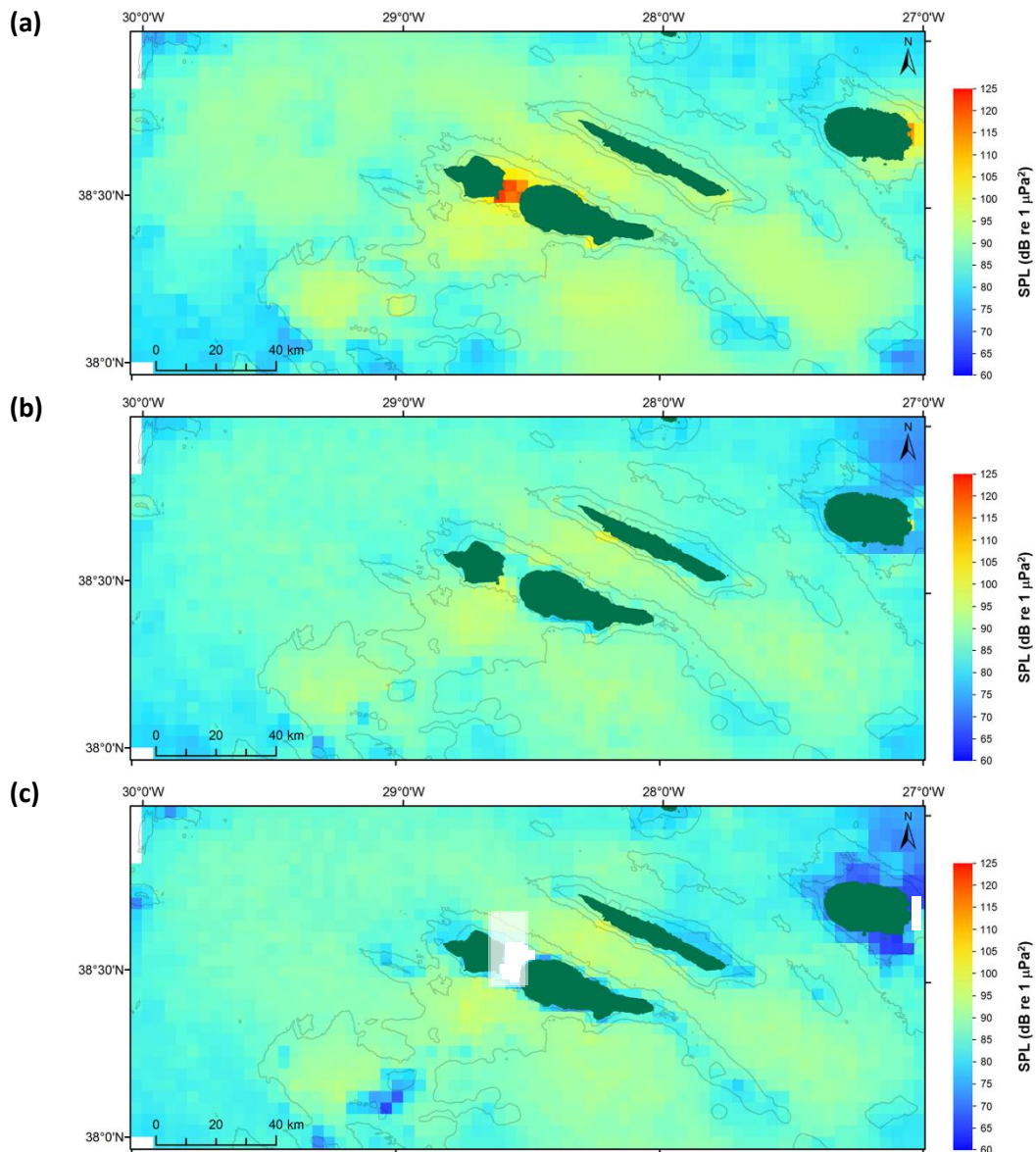


**Figure 2.** Predicted average SPL [dB re 1  $\mu\text{Pa}$ ] for all the 1/3 octave frequency bands in the interval 40–1000 Hz for the period 1-30 June 2018 at (a) 10m depth, (b) 200 m depth, and (c) 484 m depth. AIS data used to predict SPL is shown in Figure 1. Grid cells with no data are shown in white.

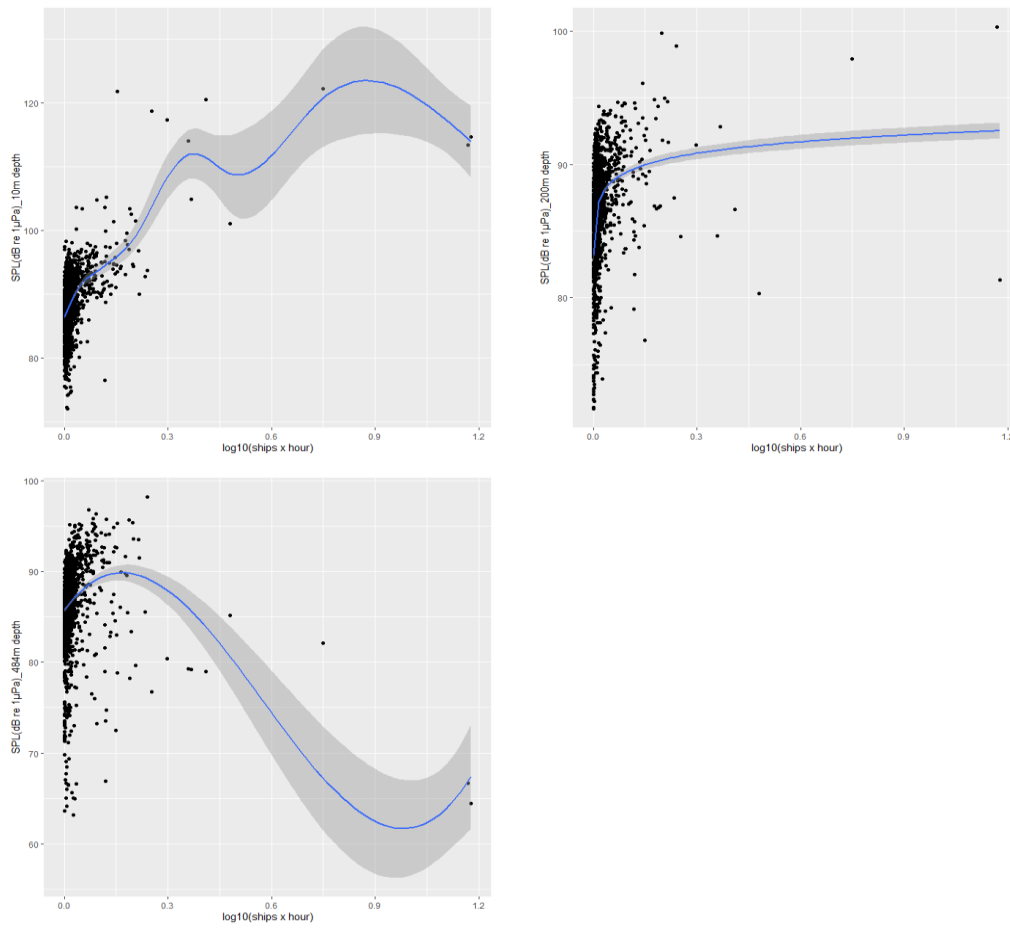


**Figure 3.** Relationship between predicted average SPL at 10m (top left), 200m (top right) and 484 m (bottom left) and shipping density for each grid cell. SPL [dB re  $1\mu\text{Pa}$ ] was estimated for all the 1/3 octave frequency bands in the interval 40–1000 Hz for the period 1-30 June 2018. Shipping density [ $\log_{10}(\text{ship} \times \text{hour} + 1)$ ] was calculated from sAIS data for the same time period. The blue line represents the best fitted non-linear model and the grey band represents the 95% confidence interval of model predictions. No attempt was made to account for autocorrelation in the data or improve model fit.

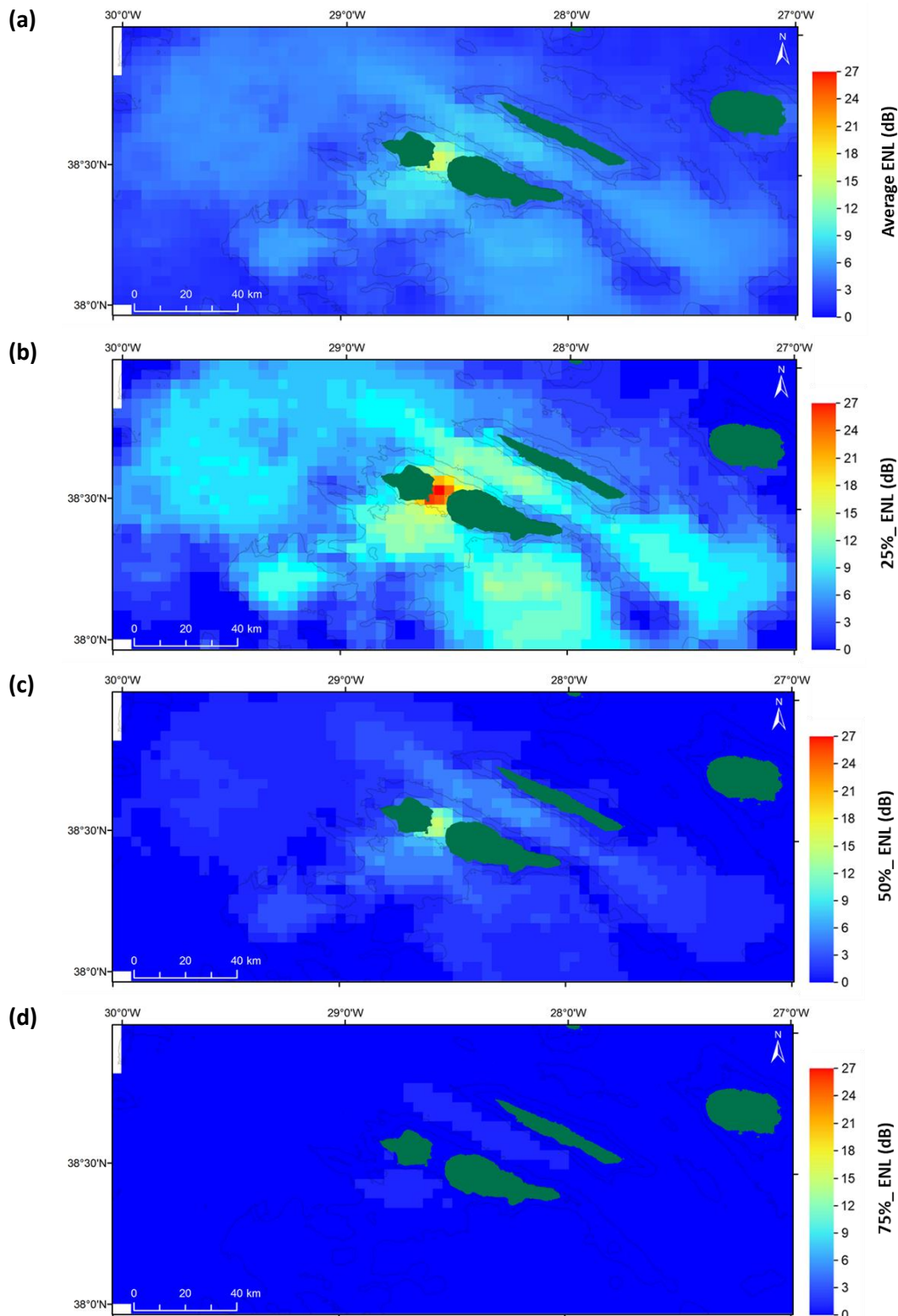


**Figure 4.** Predicted ENL [dB] at 10 m depth for all the 1/3 octave frequency bands in the interval 40–1000 Hz for the period 1–30 June 2018: **(a)** average ENL, **(b)** ENL for 25% of the month, **(c)** ENL for 50% of the month, and **(d)** ENL for 75% of the month. AIS data used to predict SPL is shown in Figure 1. Grid cells with no data are shown in white.

## 6. Comparison of risk indicators

Risk maps for the three species were built using SPL and ENL predictions at different depths, not only to reflect their distinct diving behaviour and water column use, but also to compare estimates of RI-shipping, RI-SPL and RI-ENL at

different depths (see Figures 5-7 for further information). RI was rescaled to 0-100% for mapping to facilitate comparison of relative risk among metrics within each species.

In general, risk maps based on median ENL (Figures 5c, 6c, 7c) agreed well with those based on average SPL (Figures 5b, 6b, 7b), indicating the same risk hotspots (albeit smaller), although overall RI-ENL scores were slightly lower. RI-shipping maps (Figures 5a, 6a, 7a) provided crude approximations of noise-based risk maps. Compared to risk hotspots from noise predictions, risk hotspots in RI-shipping maps were fewer, smaller and sometimes significantly displaced. In the case of Atlantic spotted dolphins, the only species for which population density in the channel Faial-Pico was  $>0$ , RI was primarily driven by the high shipping density values in the area, resulting in a single risk hotspot there. This was in clear contrast with maps of RI-SPL or RI-ENL for the species which highlighted two large areas NW and SW of Faial.

RI-shipping was significantly related to both RI-SPL and RI-ENL but these relationships were strongly non-linear for all cetacean species (Figures 5-7e,d). For a given value of RI-shipping there was a huge variation in RI values computed from noise metrics, indicating that RI-shipping was unable to capture the variability in RI-SPL and RI-ENL data (deviance explained by the models ranged between 31-55%). More importantly, RI-shipping was unable to predict the highest RI-SPL and RI-ENL values, suggesting a tendency to underestimate risk of noise exposure in locations where the relative risk predicted by noise metrics was higher. On the other hand, cells with the highest RI-shipping often did not correspond to higher RI-SPL or RI-SPL values.

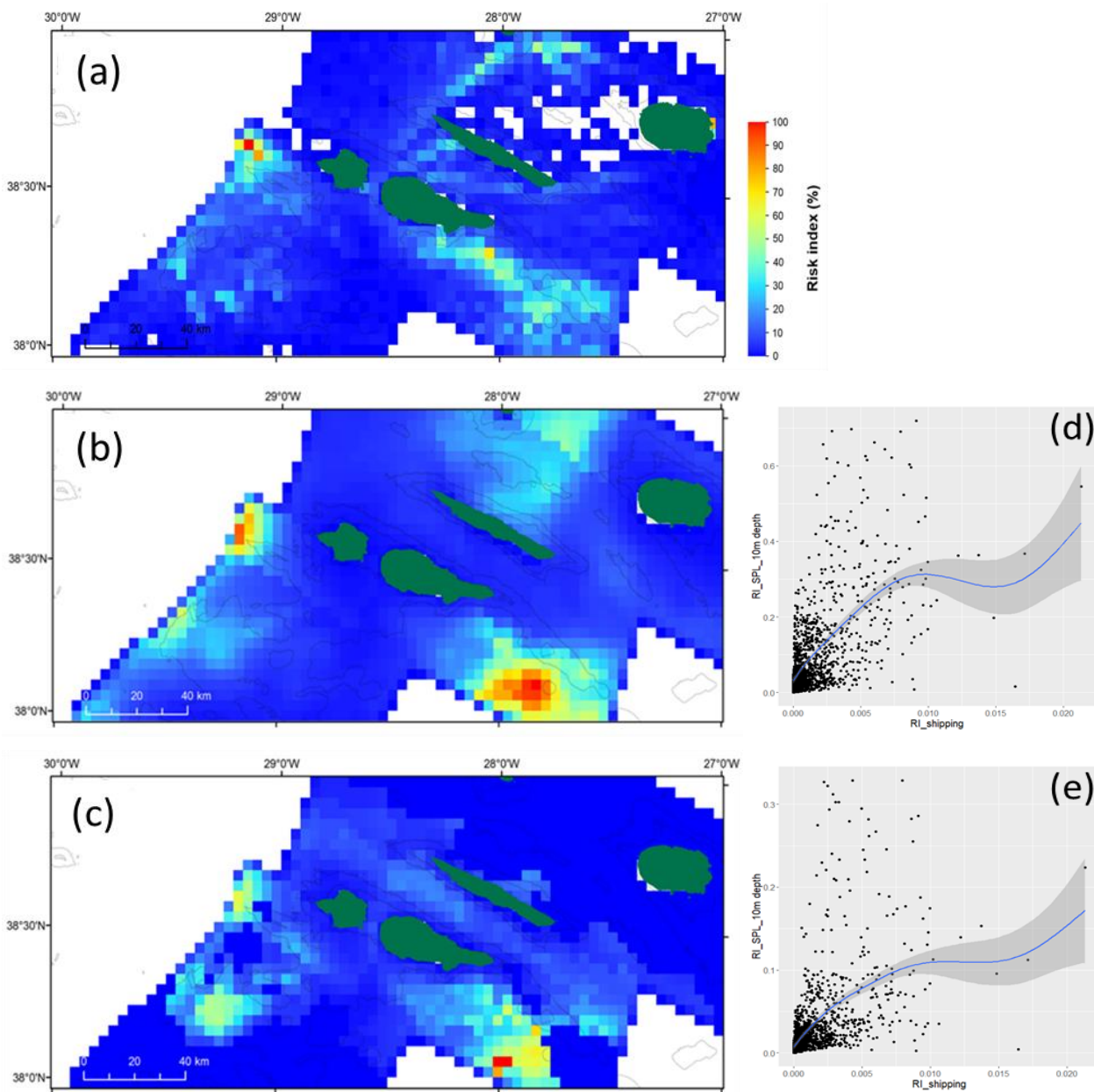


**Figure 5.** Risk maps for baleen whales (*Balaenopteridae*) during June 2018 computed from (a) shipping density, (b) average SPL at 10m depth, and (c) median ENL at 10 m depth. Baleen whale density data were from Freitas et al (2019). SPL and ENL were calculated for all one-third octave frequency bands centred in the interval 40–1000 Hz. Risk index (RI) is scaled to 0-100% in all maps. In (a) an RI of 100% corresponds to 75% of maximum baleen whale density in the area (0.17 animals/km<sup>2</sup>) and 2.9% of maximum shipping density (0.08 ship hours). In (b) an RI of 100% corresponds to the maximum baleen whale density in the area (0.22 animals/km<sup>2</sup>) and an average SPL of 87.9 dB re 1  $\mu$ Pa. In (c) an RI of 100% corresponds to 75% of the maximum baleen whale density (0.17 animals/km<sup>2</sup>) and a median ENL of 2 dB. Relationship of (d) average RI-SPL and RI-shipping, and of (e) median RI-ENL and RI-shipping. The blue line represents the best fitted generalized additive model and the grey band represent the 95% confidence interval of model predictions.

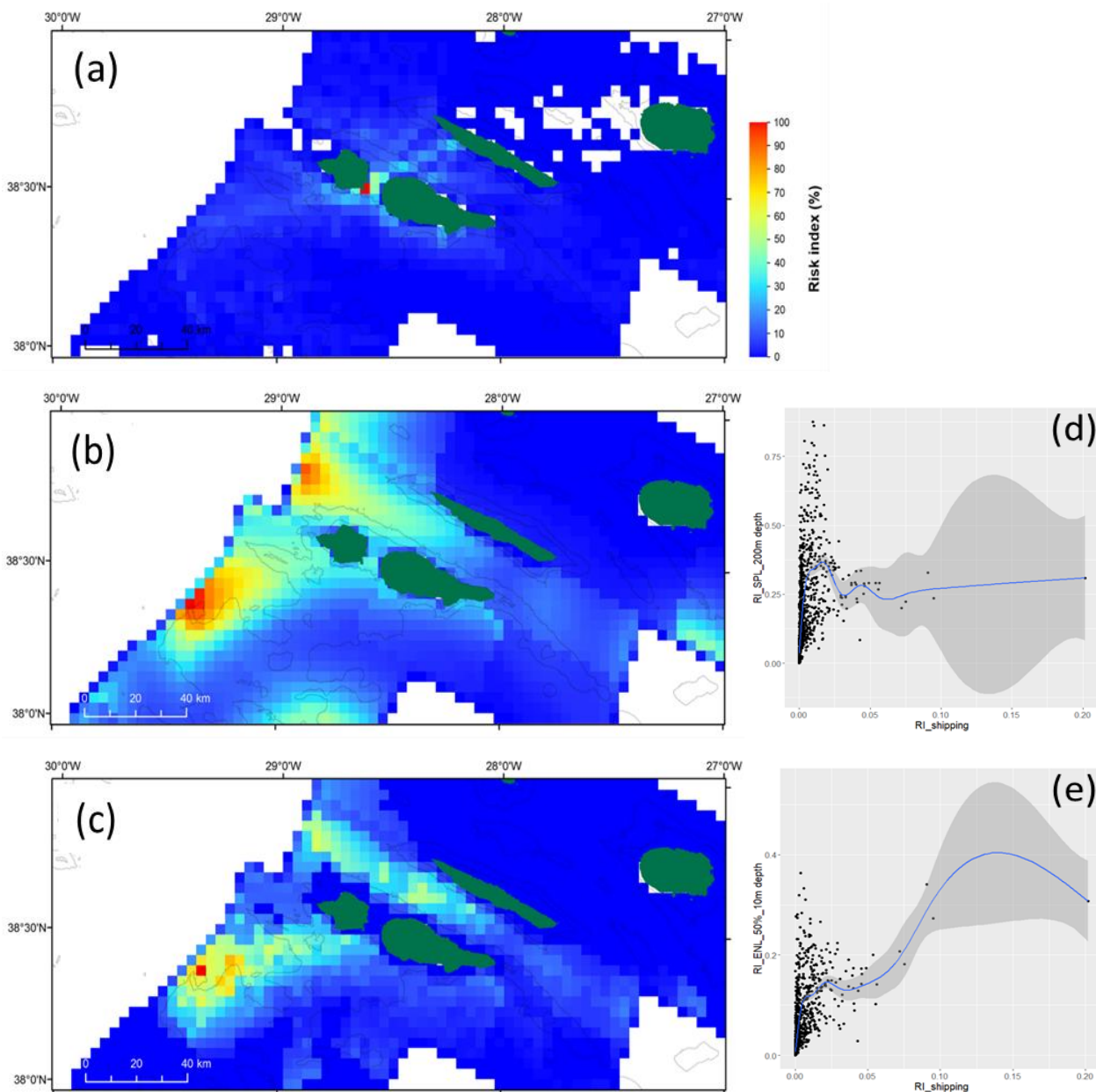


**Figure 6.** Risk maps for Atlantic spotted dolphins (*Stenella frontalis*) during June 2018 based on **(a)** shipping density, **(b)** average SPL at 200m depth, and **(c)** median ENL at 200 m depth. Atlantic spotted dolphin density data were from Freitas et al (2019). SPL and ENL were calculated for all one-third octave frequency bands centred in the interval 40–1000 Hz. Risk index (RI) is scaled to 0-100% in all maps. In (a) an RI of 100% corresponds to 33% of maximum dolphin density in the area (1.76 animals/km<sup>2</sup>) and 64% of maximum shipping density (4.62 ship hours). In (b) an RI of 100% corresponds to the maximum dolphin density in the area (5.55 animals/km<sup>2</sup>) and an average SPL of 87.9 dB re 1  $\mu$ Pa. In (c) an RI of 100% corresponds to 97% of maximum dolphin density (5.39 animals/km<sup>2</sup>) and a median ENL of 3 dB. Relationship of **(d)** average RI-SPL and RI-shipping, and of **(e)** median RI-ENL and RI-shipping. The blue line represents the best fitted generalized additive model and the grey band represent the 95% confidence interval of model predictions.

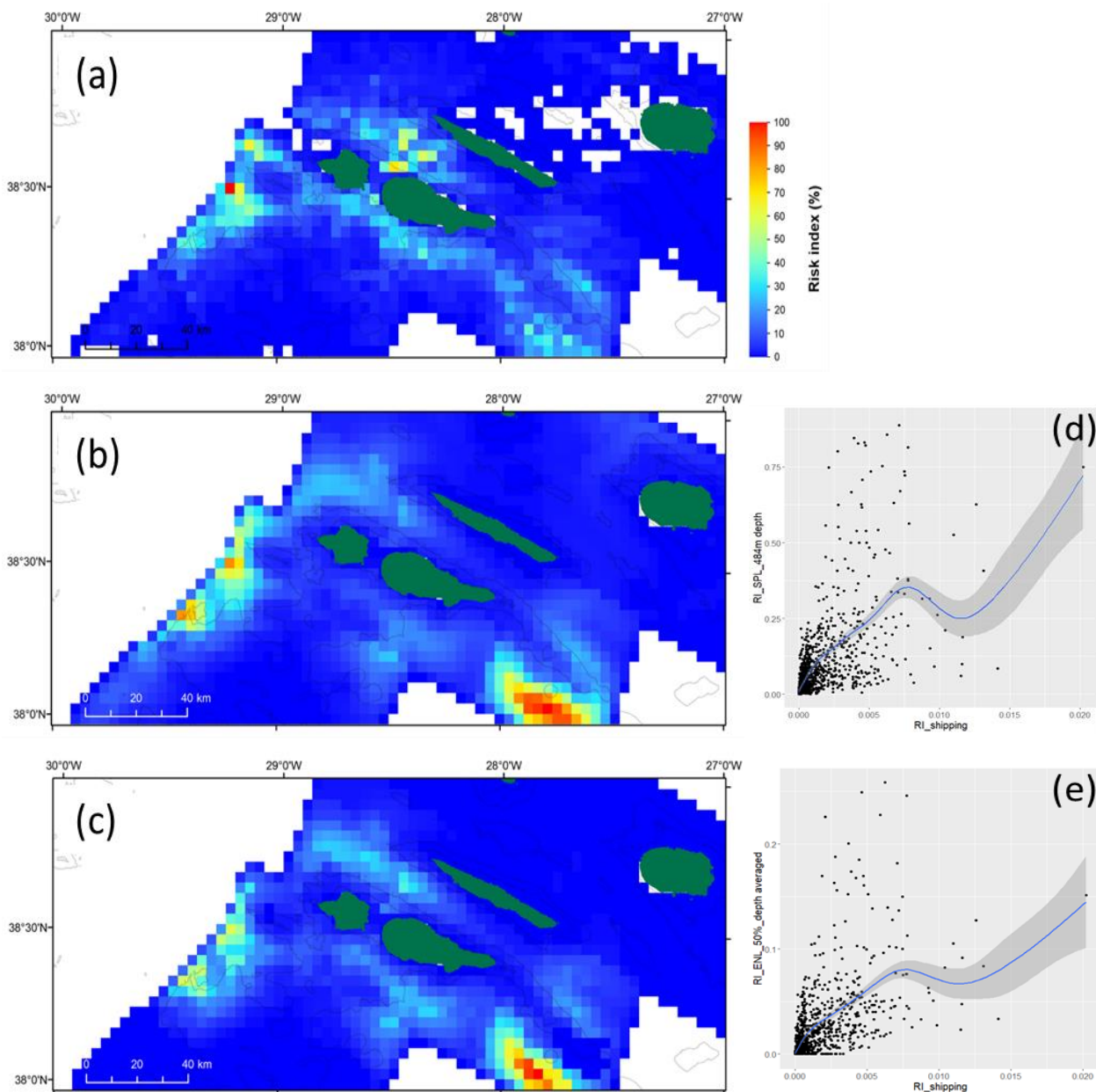


**Figure 7.** Risk maps for sperm whales (*Physeter macrocephalus*) during June 2018 based on (a) shipping density, (b) average SPL at 484m depth, and (c) median ENL averaged over all depths. Sperm whale density data were from Freitas et al (2019). SPL and ENL were calculated for all one-third octave frequency bands centred in the interval 40–1000 Hz. Risk index (RI) is scaled to 0–100% in all maps. In (a) an RI of 100% corresponds to 83% of maximum dolphin density in the area ( $0.74$  animals/ $\text{km}^2$ ) and 2.4% of maximum shipping density ( $0.07$  ship hours). In (b) an RI of 100% corresponds to the maximum sperm whale density in the area ( $0.89$  animals/ $\text{km}^2$ ) and an average SPL of  $87.2$  dB re  $1 \mu\text{Pa}$ . In (c) an RI of 100% corresponds to 95% of maximum sperm whale density ( $0.85$  animals/ $\text{km}^2$ ) and a median ENL of  $3$  dB. Relationship of (d) average RI-SPL and RI-shipping, and of (e) median RI-ENL and RI-shipping. The blue line represents the best fitted generalized additive model and the grey band represent the 95% confidence interval of model predictions.

## 7. Lessons learned and Recommendations

The results of the Azores case study illustrate some of the caveats and limitations of using measurements of shipping density based on AIS data to analyse risk from continuous anthropogenic noise.

The noisiest locations in the study area corresponded reasonably well to locations with higher density of ships. However, modelling results showed that noise propagated over large areas well beyond the shipping routes, and that propagation was strongly affected by local environmental conditions, namely bathymetry (and several other factors, including ship characteristics and speed). As a result, for most of the study area, predicted noise levels differed markedly from shipping distribution. Unsurprisingly, maps of relative risk for the three cetacean species based on shipping density and noise predictions showed different patterns of risk hotspots. Risk maps determined from shipping density yielded fewer and smaller hotspots, and sometimes hotspots from the two approaches did not overlap. Estimates of risk index based on shipping density were lower than those based on noise predictions for all cetacean species, this was especially evident in locations where the risk of noise exposure predicted by noise metrics was higher.

In this comparative analysis, it is assumed that the noise model provided an accurate representation of noise levels in the entire study area, which may not be the case, as the model was validated with field measurements from only three sites. Moreover, the comparison relied on data from a single month and a small area, and may not represent the relationship between shipping density and noise predictions over longer periods and in other areas. Additional efforts are needed to validate model predictions with field measurements from a larger number of sites and to increase the spatial extent and temporal period of the analysis.

Although preliminary, these results recommend caution in the use of shipping density as an indicator of the pressure from continuous anthropogenic noise at local scales, as it may lead to erroneous predictions of risk of exposure of marine animals to noise.

## 8. References

- Farcas A, Powell CF, Brookes KL and Merchant ND (2020). Validated shipping noise maps of the Northeast Atlantic. *Science of The Total Environment*, 735:139509
- Freitas L, Cañadas A, Servidio A, Pérez-Gil A, Pérez-Gil E, Varo-Cruz N, Silva M, Vandeperre F and Esteban R. (2019). A-MB-TR2 – Technical Report - Sub-programmes Abundance of Oceanic Cetaceans (MM) and Loggerhead Census (MT)- Oceanic. MISTIC SEAS II - Applying a sub-regional coherent and coordinated approach to the monitoring and assessment of marine biodiversity in Macaronesia for the second cycle of the MSFD (11.0661/2017/750679/ SUB/ENV.C2).
- GEBCO Bathymetric Compilation Group (2020). The GEBCO 2020 Grid - a continuous terrain model of the global oceans and land., 2020. Medium: Network Common Data Form Version Number: 1 type: dataset.
- Kuperman WA, Porter MB and Perkins JS. (1991). Rapid computation of acoustic field in three dimensional ocean environments. *Journal of Acoustical Society of America*, 89:125–133.
- Mackenzie K. (1981). Nine-term equation for sound speed in the oceans. *Journal of the Acoustical Society of America*, 70: 807–812.
- Maglio A, Soares C, Bouzidi M, Zabel F, Souami Y and Pavan G. (2015). Mapping Shipping noise in the Pelagos Sanctuary (French part) through acoustic modelling to assess potential impacts on marine mammals. *Sci. Rep. Port-Cros Natl. Park*, 185: 167–185.
- McKenna MF, Ross D, Wiggins SM and Hildebrand JA. (2012). Underwater radiated noise from modern commercial ships. *Journal of the Acoustical Society of America*, 131: 92–103.
- Merchant ND, Farcas A and Powell CF. (2018a) Acoustic metric specification. Report of the EU INTERREG Joint Monitoring Programme for Ambient Noise North Sea (JOMOPANS).
- Merchant ND, Faulkner RC and Martinez R. (2018b). Marine noise budgets in practice. *Conservation Letters* 11, e12420.
- Porter MB and Reiss EL. (1984). A numerical method for ocean acoustic normal modes. *Journal of the Acoustical Society of America*, 76: 244.

- Soares C, Duarte RJ, Silva MA, Romagosa M and Jesus SM. (2020a). Shipping noise in the Azores: a threat to the Faial-Pico cetacean community? *Proceedings of Meetings on Acoustics*, 40(1): 070012.
- Soares C, Duarte R, Zabel F, Silva MA and Jesus SM. (2020b). Shipping noise predictions from AIS in the Faial-Pico area, Azores archipelago. *Global OCEANS 2020 - Online Proceedings*, pp. 1-6.
- Soares C, Zabel F and Jesus SM. (2015). A shipping noise prediction tool. *OCEANS 2015 – Genova*, pp. 1-7.
- Southall BL, Finneran JJ, Reichmuth C, Nachtigall PE, Ketten DR, Bowles AE et al. (2019). Marine mammal noise exposure criteria: updated scientific recommendations for residual hearing effects. *Aquatic Mammals* 45, 125–232.
- van Oostveen M, Barbé D and Kwakkel J. (2020). OSPAR candidate indicator ambient underwater sound. Technical Report BH2849WATRP2003261655.

## Appendix I

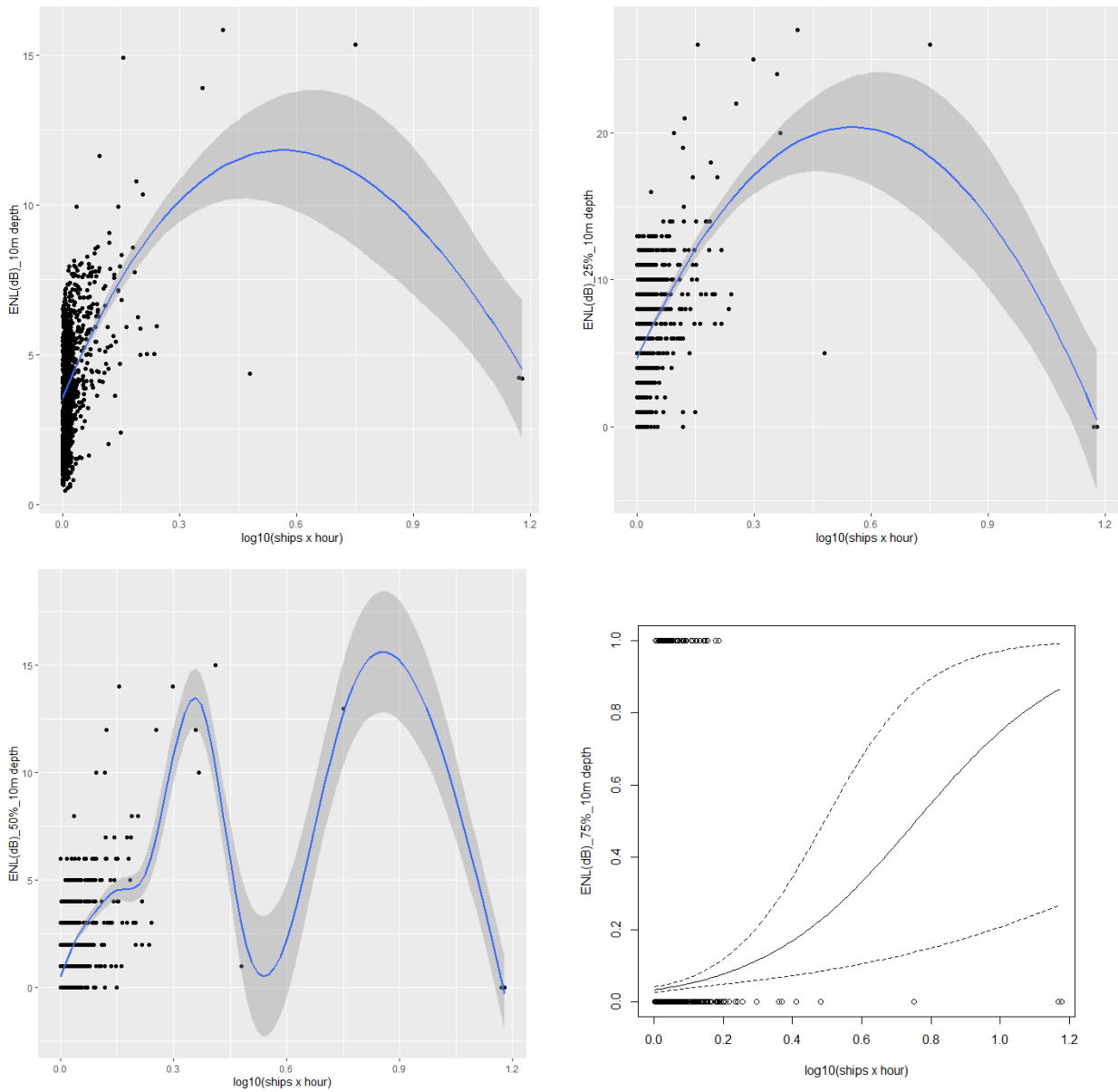


**Figure A.** Relationship between predicted average ENL (top left), median ENL (top right), ENL exceeded for 25% of the time (percentile 75<sup>th</sup>) (bottom left), and ENL exceeded for 75% of the time (percentile 25<sup>th</sup>) (bottom right) and shipping density for each grid cell. ENL [dB] was estimated for all the 1/3 octave frequency bands in the interval 40–1000 Hz for the period 1–30 June 2018. Shipping density [ $\log_{10}(\text{ship} \times \text{hour} + 1)$ ] was calculated from sAIS data for the same time period. The blue/black line represents the best fitted non-linear model and the grey band/dashed lines represent the 95% confidence interval of model predictions. No attempt was made to account for autocorrelation in the data or improve model fit.